

# The X-ray luminosity–velocity dispersion relation in the REFLEX cluster survey

A. Ortiz-Gil,<sup>1,2\*</sup> L. Guzzo,<sup>2</sup> P. Schuecker,<sup>3</sup> H. Böhringer<sup>3</sup> and C. A. Collins<sup>4</sup>

<sup>1</sup>*Observatorio Astronómico, Universidad de Valencia, Aptdo. 22085, Valencia E-46071, Spain*

<sup>2</sup>*INAF, Osservatorio Astronomico di Brera, Merate I-23807, Italy*

<sup>3</sup>*Max-Planck-Institut für Extraterre. Physik, D-85740 Garching, Germany*

<sup>4</sup>*Astrophysics Research Institute, Liverpool John Moores University, Twelve Quays House, Egerton Wharf, Birkenhead L14 1LD*

Accepted 2003 November 3. Received 2003 October 29; in original form 2003 June 11

## ABSTRACT

We present an estimate of the bolometric X-ray luminosity–velocity dispersion ( $L_x$ – $\sigma_v$ ) relation measured from a new, large and homogeneous sample of 171 low-redshift, X-ray selected galaxy clusters. The linear fitting of  $\log(L_x)$ – $\log(\sigma_v)$  gives  $L_x = 10^{32.72 \pm 0.08} \sigma_v^{4.1 \pm 0.3} \text{ erg s}^{-1} h_{50}^{-2}$ . Furthermore, a study of 54 clusters, for which the X-ray temperature of the intracluster medium  $T$  is available, allows us to explore two other scaling relations,  $L_x$ – $T$  and  $\sigma_v$ – $T$ . From this sample we obtain  $L_x \propto T^{3.1 \pm 0.2}$  and  $\sigma_v \propto T^{1.00 \pm 0.16}$ , which are fully consistent with the above result for  $L_x$ – $\sigma_v$ . The slopes of  $L_x$ – $T$  and  $\sigma_v$ – $T$  are incompatible with the values predicted by self-similarity ( $L_x \propto T^2 \propto \sigma_v^4$ ), thus suggesting the presence of non-gravitational energy sources heating up the intracluster medium, in addition to the gravitational collapse, in the early stages of cluster formation. On the other hand, the result on  $\log(L_x)$ – $\log(\sigma_v)$  supports the self-similar model.

**Key words:** galaxies: clusters: general – galaxies: fundamental parameters – cosmology: observations.

## 1 INTRODUCTION

Galaxy clusters are dark matter haloes which form mainly through the process of gravitational collapse, and so they are expected to be self-similar; small clusters or galaxy groups must be scaled-down versions of the more massive systems. Self-similarity predicts a series of relationships between different cluster observables such as X-ray luminosity  $L_x$ , mass  $M$ , temperature  $T$  and galaxy velocity dispersion  $\sigma_v$ , which are the same in all systems (Kaiser 1991).

The radial velocity dispersion  $\sigma_v$  of the galaxies in a cluster probes the depth and shape of the potential well, assuming that the luminous matter traces reasonably well the dark matter in clusters. Moreover, the intracluster gas emits X-rays through a process of thermal bremsstrahlung and its bolometric luminosity  $L_x$  is found to be strongly correlated with  $\sigma_v$ , as both gas and galaxies share a common potential well (Solinger & Tucker 1972). Also, because the X-ray emission can be well modelled by thermal emission of a hot, optically thin plasma,  $L_x$  and the plasma temperature  $T$  must be correlated. Finally, because galaxies are embedded in the intracluster medium (ICM), a correlation is also expected between the gas temperature  $T$  and the galaxies velocity dispersion  $\sigma_v$ .

Self-similar models consider that the only energy source in the cluster comes from the gravitational collapse, predicting the follow-

ing scaling relations:  $L_x \propto T^2 \propto \sigma_v^4$ . Whereas there seems to be a general agreement between different measurements that  $L_x \propto T^{\sim 3}$ , the measurement of  $L_x$ – $\sigma_v$  has given contradictory results so far. Some authors have found that  $L_x \propto \sigma_v^4$  indeed, although with quite large measurement errors or rather small data samples, while others find slopes larger than 4 (see Table 1). Part of the differences in the results could come from different ways of selecting the sample, with a preference for regular clusters in some of these surveys.

It has also been suggested that clusters and groups do not follow the same  $L_x$ – $\sigma_v$  scaling relation, the latter being flatter than the former (e.g. Dell’Antonio, Geller & Fabricant 1994; Mahdavi et al. 2000; Xue & Wu 2000). However, there are other measurements contrary to that conclusion (Mulchaey & Zabludoff 1998; Mahdavi & Geller 2001).

For more distant clusters ( $z$  between  $\sim 0.15$  and  $\sim 0.6$ ) there is some evidence that the slope is also  $> 4$  (Borgani et al. 1999; Girardi & Mezzetti 2001), although only small samples are available at the moment, and more data are needed to reduce the error bars.

There is a clear need of new measurements performed on large samples (more than 100 clusters), selected from a homogeneous data set. The largest cluster (not group) samples available up to date, on which this kind of study has been performed, are literature compilations combining data from different authors and/or instruments (for example Xue & Wu 2000; Mahdavi & Geller 2001). The present work comes to partially fill this gap, as we have a large homogeneous subsample of clusters selected from the *ROSAT*–European Southern

\*E-mail: amelia.ortiz@uv.es

**Table 1.** Compilation of literature values obtained for  $a$  and  $b$  in the relation  $\log(L_x) = a + b \log(\sigma_v)$ . The number of clusters that entered the computation is also shown, together with some information about the sample and the cluster selection method.  $L_x$  is in units of  $\text{erg s}^{-1}$  and  $\sigma_v$  is in  $\text{km s}^{-1}$ . All of these, except for Quintana & Melnick (1982), make use of bolometric luminosities. Only White, Jones & Forman (1997) remove cooling flow clusters from the sample. Multicomponent clusters are explicitly removed in Girardi & Mezzetti (2001), Borgani et al. (1999) and in this work (b). This work (c) is the result obtained when using a volume-limited sample.

Reference	$b$	$a$	No. clusters	Flux-limited sample	Selection method
Edge & Stewart (1991)	$2.90 \pm 0.19$	$36.60 \pm 0.55$	23	No	Optical
Quintana & Melnick (1982)	$3.7 \pm 0.4$	–	31	No	Optical
Mulchaey & Zabludoff (1998)	$4.29 \pm 0.37$	$31.61 \pm 1.09$	38	No	Optical and X-ray
Mahdavi & Geller (2001)	$4.4^{+0.7}_{-0.3}$	$31.8^{+0.9}_{-2.0}$	280	No	Optical and X-ray
Girardi & Mezzetti (2001)	$4.4^{+1.8}_{-1.0}$	$29.4^{+3.0}_{-5.4}$	51	No	Optical and X-ray
Borgani et al. (1999)	$5.1^{+1.2}_{-0.8}$	$27.8^{+3.0}_{-2.2}$	53	Yes	X-ray
Xue & Wu (2000)	$5.30 \pm 0.21$	$28.32 \pm 0.61$	197	No	Optical and X-ray
White et al. (1997)	$5.36 \pm 0.16$	$39.3^{+0.13}_{-0.9}$	14	No	Optical
This work (a)	$4.1 \pm 0.3$	$32.72 \pm 0.08$	171	Yes	X-ray
This work (b)	$4.2 \pm 0.4$	$32.41 \pm 0.10$	123	Yes	X-ray
This work (c)	$3.2 \pm 0.3$	$35.16 \pm 0.09$	51	Yes	X-ray

Observatory (ESO) flux-limited X-ray (REFLEX) selected cluster catalogue, built under well-defined selection criteria.

The structure of this paper is as follows. In Section 2 we give a brief introduction to the REFLEX catalogue and the way in which the subsample in this paper has been selected. Section 3 illustrates in detail the process of the  $L_x$  and  $\sigma_v$  measurements, which lead to the fitting of the  $\log(L_x)$ – $\log(\sigma_v)$  in Section 4. In Section 5.1 we propose the removal of those clusters in the sample which are multiple systems. In Section 5 we analyse possible biases due to the nature of the selected sample. A study of the  $L_x$ – $T$  and  $\sigma_v$ – $T$  relation follows in Section 6, and we finish with a summary in Section 7. We are assuming  $H_0 = 50 \text{ km s}^{-1} \text{ Mpc}^{-1}$  in a flat universe with  $\Omega_\Lambda = 0.7$ .

## 2 THE DATA

The REFLEX cluster survey (Böhringer et al. (2001); Böhringer et al. in preparation; Guzzo et al., in preparation) has identified and measured successfully the redshift for all southern galaxy clusters (at galactic latitude  $|b| > 20^\circ$ ) down to a flux limit  $f_x > 3 \times 10^{-12} \text{ erg s}^{-1} \text{ cm}^{-2}$  in the *ROSAT* All-Sky Survey. This sample has already provided us with results concerning the measurement of the cluster X-ray luminosity function at low redshift (Böhringer et al. 2002), the power spectrum (Schuecker et al. 2001a), the spatial correlation function (Collins et al. 2000), the measurement of  $\Omega_m$  and  $\sigma_8$  (2003a) or the measurement of the equation of state parameter  $w$  of the dark energy (Schuecker et al. 2003b), among others. A detailed description of the sample construction can be found in Böhringer et al. (2001).

REFLEX is an X-ray selected sample and the first compilation of the REFLEX catalogue includes 452 clusters down to a flux limit of  $3 \times 10^{-12} \text{ erg s}^{-1} \text{ cm}^{-2}$  in the *ROSAT* energy band from 0.1 to 2.4 keV. The survey covers a total area in the sky of 4.24 sr. Two regions corresponding to the Magellanic clouds and the Galactic plane have been excluded because of the difficulties in identifying clusters of galaxies in these densely crowded regions, as well as some strips of the sky which were not observed by *ROSAT* due to power-off of the detector when the satellite was crossing the Earth's radiation belts – see fig. 2 in Böhringer et al. (2001), for a survey exposure map.

Optical follow-up has been performed through long-slit and multi-object spectroscopy at the 1.5-m, 2.2-m and 3.6-m ESO telescopes at La Silla (Chile) during a series of observing campaigns, which started back in 1991. We complement our sample of galaxy redshifts by looking into the literature, using the NASA/IPAC Extragalactic Database (NED), and adding those redshifts already published for the previously known clusters.

The cluster membership of each individual galaxy has been decided based on the search for velocity peaks in the velocity distribution of the galaxies observed in the field. All galaxies were assigned the same weight in the computation of the cluster's median redshift because in most cases not enough photometric material is available to give proper weights (i.e. to identify a real central dominant galaxy). Anyway, bright cluster galaxies (if present) were used to decide on the main redshift of the system when it showed multiple velocity peaks in the redshift histogram along the line of sight. In other cases, the choice among multiple velocity peaks was decided taking into account the correlation between the peak position and the X-ray emission centre and also the strength of the peak. Finally, other clusters ended up being split into different systems when multiple X-ray emission centres associated to them were detected.

We have selected from REFLEX those clusters with more than seven measured galaxy redshifts (see Fig. 1), including only galaxies at a maximum projected distance from the cluster centre of  $0.5 h_{50}^{-1} \text{ Mpc}$ , due to the lack of data at larger distances from the cluster centre. Outliers in the velocity space were rejected by applying the three-sigma clipping method; galaxies with velocity differences with the cluster centre velocity larger than three times the measured velocity dispersion were not used in the subsequent iterations to avoid possible contamination by foreground/background objects. By following this procedure we end up with 171 clusters out of the 452 in the whole catalogue. It is a low-redshift sample, the median redshift being 0.076. Only 14 clusters have  $z$  above 0.2 (see Fig. 2).

## 3 MEASUREMENT OF $L_x$ AND $\sigma_v$

### 3.1 Bolometric X-ray luminosity $L_x$

Counts in the *ROSAT* images were measured using the growth curve analysis (GCA) and then converted into fluxes, as described in

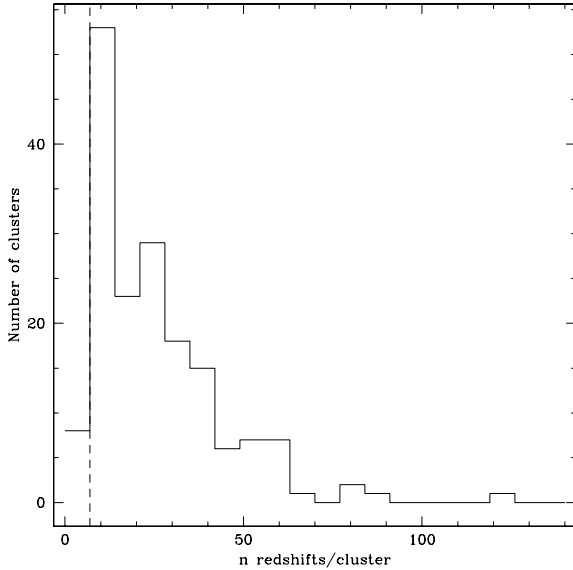


**Figure 1.** Distribution of the number of redshifts per cluster in the 171 subsample of the REFLEX catalogue which we study in this paper. The dashed vertical line shows the limit of seven redshifts per cluster imposed to select the clusters for which  $\sigma_v$  is measured.

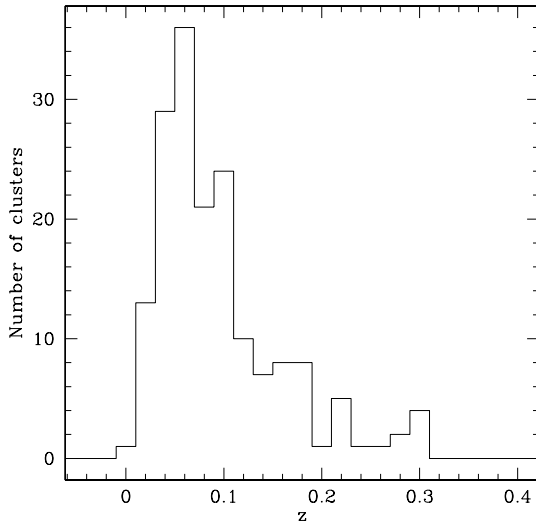


**Figure 2.** Redshift distribution of the 171 clusters in the selected sample from the REFLEX catalogue.

Böhringer et al. (2001). Luminosities have first been transformed into the *ROSAT* rest-frame band (0.1–2.4 keV) (see Böhringer et al. 2002, for details) and afterwards into bolometric luminosities. We assumed a MEKAL spectral model with an ICM metallicity of  $0.3 Z_{\odot}$  (Anders & Grevesse 1989). We used XSPEC (Arnaud 1996) to obtain the relation between the luminosity in the 0.1–2.4 keV band and the bolometric one, as a function of the cluster temperature (see Böhringer et al., in preparation, for a detailed conversion table), which was computed from the velocity dispersions assuming the empirical relation between  $\sigma_v$  and  $T$  measured by Girardi et al. (1996).

### 3.2 Radial velocity dispersion $\sigma_v$

The radial velocity dispersions  $\sigma_v$  have been computed by means of the biweight estimator of central location and scale (within RO-

STAT by Beers, Flynn & Gebhardt 1990). This estimator was first suggested by Tuckey in Andrews et al. (1972) as a better way to study non-Gaussian or contaminated normal distributions than the Gaussian estimators (mean and standard deviation). The biweight location estimator belongs to the family of estimators known as  $M$  estimators of location. It works by minimizing a function of the deviations of each observation from the estimate of location and has the advantage that it does not assume an underlying Gaussian distribution, which in our case means to have a perfectly relaxed cluster and might not be the case in most of the sample. It is less affected by points in the wings of the distribution and is robust for a broad range of non-Gaussian underlying populations.

We used the biweight estimator of central location and the gap-  
per estimator of scale (based on the gaps between order statistics; Wainer & Thissen 1976) when the number of redshifts available in the cluster was  $7 \leq N_z \leq 10$ . For  $N_z > 10$  the biweight estimator was chosen for both location and scale. Errors were obtained in all cases by jackknifing of the biweight. The choice of the different estimators has been made on the basis of the tests carried out by Beers et al. (1990) for samples with different numbers of data points. The usual cosmological correction and the correction for velocity errors (Danese, de Zotti & di Tullio 1980) were also applied. The whole procedure was performed iteratively until the results converged.

The clusters with the larger errors in the velocity dispersion estimate are among those for which  $N_z \leq 10$ .

One source of concern is the fact that we are computing  $\sigma_v$  using galaxies which are quite close to the cluster centre, at distances less than  $0.5 h_{50}^{-1}$  Mpc (median distance is  $0.04 h_{50}^{-1}$  Mpc). Girardi et al. (1996) find that the value of  $\sigma_v$  is a function of the distance to the cluster centre, and it reaches a stable value when galaxies at a projected distance of  $\sim 1 h_{50}^{-1}$  Mpc are considered. At smaller distances,  $\sigma_v$  does not show a constant behaviour; sometimes it raises up, sometimes it goes down, and in some cases it remains stable. So, in a large sample such as ours we expect that this effect will cancel out. From our current data, it is not possible to determine  $\sigma_v$  at clustercentric distances larger than  $0.5 h_{50}^{-1}$  Mpc.

## 4 THE $L_x - \sigma_v$ RELATION

A power law was fitted to the  $\log(L_x) - \log(\sigma_v)$  relation by means of the orthogonal distance regression (ODR) method (Boggs et al. 1992), which takes into account errors on both variables. We took the data in units of  $L_x/10^{45} \text{ erg s}^{-1}$  ( $L_{45}$ ) and velocity dispersions in units of  $\sigma_v/500 \text{ km s}^{-1}$  ( $\sigma_{500}$ ), that is, we put the origin of coordinates more or less at the centre of the data point cloud to help the model find the right  $Y$ -axis intercept. We will use these units throughout the paper, but for Table 1, where we quote  $L_x$  in  $\text{erg s}^{-1}$  and  $\sigma_v$  in  $\text{km s}^{-1}$  for comparison purposes with the works referenced there. The best fit to  $\log(L_{45}) - \log(\sigma_{500})$  is found to be (see Fig. 3)

$$\log(L_{45}) = (-1.34 \pm 0.08) + (4.1 \pm 0.3) \times \log(\sigma_{500}) \text{ erg s}^{-1} h_{50}^{-2}. \quad (1)$$

The Spearman rank correlation coefficient for this sample is  $r_s = 0.51$  and the probability that a random distribution had this value of  $r_s$  or larger by chance is  $P \leq 2.6 \times 10^{-11}$ .

The distribution of errors in the sample has been assumed to be normal in the ODR fitting. To test for this assumption, we have performed a maximum likelihood analysis with sigma clipping to find which is the best-fitting Gaussian to the actual error distribution in  $X$ . As errors in  $X$  are far larger than errors in  $Y$ , we can neglect the effect of the latter. We find that the best Gaussian has central

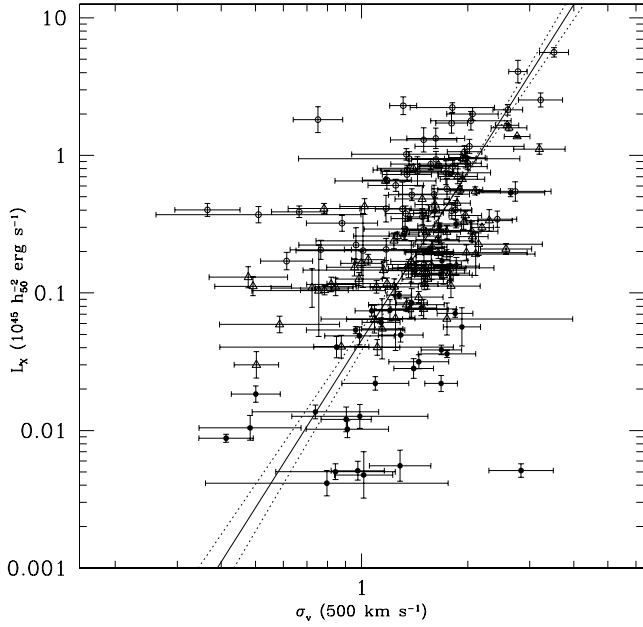


**Figure 3.** Bolometric X-ray luminosity  $L_x$  versus radial velocity dispersion  $\sigma_v$  for a REFLEX sample of 171 clusters. The linear fit gives a log slope of  $4.1 \pm 0.3$ , and the dashed lines are the one-sigma errors. Filled circles correspond to clusters at redshift  $z \leq 0.05$ , open triangles are clusters with  $0.05 < z \leq 0.1$  and open circles are clusters at  $z > 0.1$ .

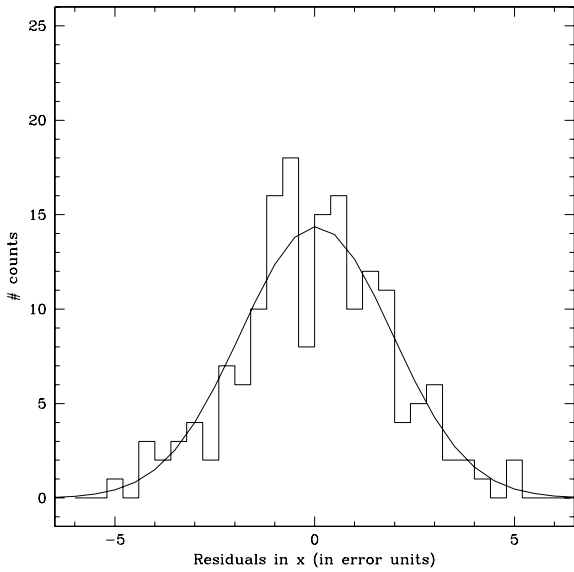


**Figure 4.** Distribution of residuals along the  $X$ -axis in the 171 cluster sample. We also show the corresponding maximum likelihood normal distribution. The distribution of residuals is well approximated by a Gaussian distribution, with central location at  $\bar{x} = 0.04$  and standard deviation  $\sigma = 1.9$ .

location  $\bar{x} = 0.04$  and standard deviation  $\sigma = 1.9$  (Fig. 4). The error distribution along the  $X$ -axis is thus reasonably Gaussian.

We can also perform a crude estimate of the intrinsic dispersion of the sample,  $\Sigma_{\text{int}}$ ,

$$\Sigma_{\text{int}} = \sqrt{(\sigma_{\text{obs}}^2 - \sigma_{\text{meas}}^2)}, \quad (2)$$

in error units.  $\sigma_{\text{obs}}$  is the best-fitting Gaussian  $\sigma$  parameter as found above for the current error distribution, i.e.  $\sigma_{\text{obs}} = 1.9$ .  $\sigma_{\text{meas}}$  is the

parameter of the error distribution in the ideal case in which only the measurement errors are responsible for the dispersion in the data, which would be a Gaussian with  $\sigma = 1$ . We find  $\Sigma_{\text{int}} = 1.62$  in error units, that is, the intrinsic dispersion of the sample is slightly larger than the dispersion due to the errors in the data. To see what this means in terms of physical units, let us assume that a typical value of the error in the velocity dispersion is the median of the error distribution,  $\Sigma_{\text{typ}} = 120 \text{ km s}^{-1}$ . The intrinsic dispersion is then

$$\sigma_{\text{int}} = 1.62 \Sigma_{\text{typ}} = 195 \text{ km s}^{-1}. \quad (3)$$

Finally, to test for the stability of the fitting, we repeated it by removing those points with an error in the velocity dispersion larger than 30 per cent of their value. We find

$$\log(L_{45}) = (-1.38 \pm 0.09) + (4.2 \pm 0.3) \log(\sigma_{500}), \quad (4)$$

thus showing the robustness of the fitting against the presence of large errors in  $\sigma_v$ .

We may also worry about the small number of redshifts (seven at minimum) with which we are computing  $\sigma_v$  in some clusters. We have repeated the fit, this time taking only clusters for which  $\sigma_v$  had been determined from at least 30 individual redshifts. In this way, we are left with a sample of only 57 clusters. The best-fitting relation is

$$\log(L_{45}) = (-1.44 \pm 0.12) + (4.2 \pm 0.4) \log(\sigma_{500}), \quad (5)$$

which is in agreement at the one-sigma confidence level with the fit obtained for the whole sample. Fig. 5 shows the best fit found.

The best-fitting Gaussian to the error distribution in  $X$  is centred at  $\bar{x} = 0.3$  and has standard deviation  $\sigma = 1.9$ . This gives a value for the intrinsic dispersion of  $\Sigma_{\text{int}} = 195 \text{ km s}^{-1}$ .

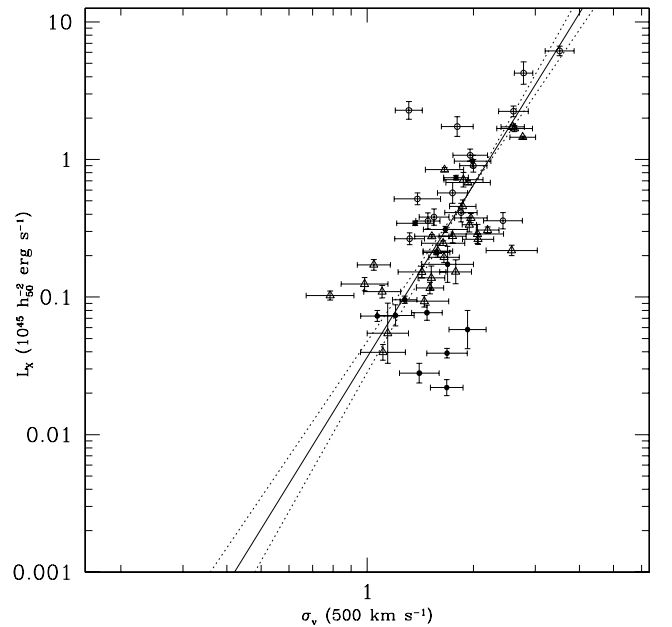


**Figure 5.** Bolometric X-ray luminosity  $L_x$  versus radial velocity dispersion  $\sigma_v$  for a REFLEX sample of 57 clusters for which more than 30 galaxy redshifts entered the  $\sigma_v$  computation. The linear fit gives a log slope of  $4.1 \pm 0.4$ , and the dashed lines are the one-sigma errors. Filled circles correspond to clusters at redshift  $z \leq 0.05$ , open triangles are clusters with  $0.05 < z \leq 0.1$  and open circles are clusters at  $z > 0.1$ .

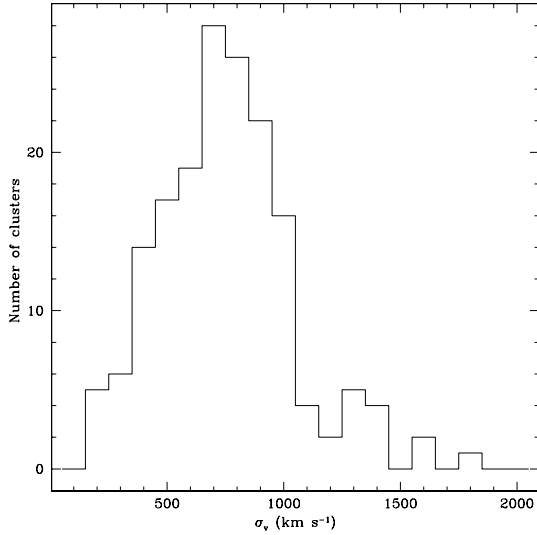


Figure 6. Velocity dispersion distribution in the cluster sample.

## 5 DISCUSSION

Self-similarity in the purely gravitational hierarchical scenario of structure formation implies that for galaxy clusters  $L_x \propto T^2 \propto \sigma_v^4$ . Although several authors have found a good agreement between this prediction and their measurements for the  $L_x - \sigma_v$  relation, others have found steeper values (see Table 1).

Our value of  $a = 4.1 \pm 0.3$  is in good agreement with the slope measured by Quintana & Melnick (1982), Mulchaey & Zabludoff (1998), Mahdavi & Geller (2001) and Girardi & Mezzetti (2001). As for the intercepts, our result is compatible with Mulchaey & Zabludoff (1998) and Mahdavi & Geller (2001) at about the one-sigma confidence level.

From Fig. 6 we can see that our sample is mostly populated by clusters and groups are practically absent, if we consider as ‘groups’ those systems with  $\sigma_v < 340 \text{ km s}^{-1}$  (following the criterion used by Mahdavi et al. 2000). More specifically, only 11 out of the 171 systems are groups. Some authors (e.g. Dell’Antonio et al. 1994; Helsdon & Ponman 2000; Mahdavi et al. 2000; Xue & Wu 2000) have found that the scaling laws are different for clusters and groups. In particular, they find that clusters show a steeper slope in the  $L_x - \sigma_v$  relation. Unfortunately, we cannot derive a meaningful  $L_x - \sigma_v$  relation for groups from our sample, due to the small number of groups observed.

The complexity involved in the measurements of  $\sigma_v$  and  $L_x$  (because of the presence of substructures, cooling flows, and other physical phenomena), the largely unknown intrinsic dispersion of their relationship, and the use of different fitting methods could explain the different results reached by the different works. For example, Xue & Wu (2000) illustrate the different results obtained by using ODR regression and ordinary least-squares (OLS) regression in the analysis.

### 5.1 A sample free from clusters with substructures

Substructures in clusters constitute a problem in the radial velocity dispersion estimates, as the different components show different  $\sigma_v$  and an estimate of a single  $\sigma_v$  for the cluster may not be meaningful. We cannot make a reliable study of the substructures in our clusters as in many cases we do not have enough redshifts to perform it. The sensitivity for substructure detection depends strongly on the

number of galaxies with measured redshift available for each cluster. In our sample, though, we have large differences in the number of galaxies per cluster and trying to detect substructure is not feasible.

In a paper by Schuecker et al. (2001b) they identify the clusters in the REFLEX sample which show multiple components in the X-ray emission. When we take those clusters out from our sample, we end up with 123 clusters. In this case we have

$$\log(L_{45}) = (-1.28 \pm 0.10) + (4.2 \pm 0.4) \log(\sigma_{500}), \quad (6)$$

which is again in very good agreement with that obtained for the whole sample.

This result shows that our sample is not largely affected by the problems of substructure, probably because we are selecting galaxies very close to the X-ray peak emission, that is, to the central potential well, where we would expect that the strength of the gravitational potential will erase any substructures which might be present. Even in the case of redshifts taken from the literature (see Section 5.2) we have not considered galaxies farther than  $0.5 h_{50}^{-1} \text{ Mpc}$ , to be consistent with the characteristics of our own data.

### 5.2 Inhomogeneous redshift data sources

The galaxy redshifts used in this work come from three different sources. When a cluster was already known and well studied, redshifts were taken from the literature, possibly from different authors too. When a cluster was already known but had little data available in the literature, we took our own redshifts in order to secure and/or improve the cluster redshift. Finally, in the case of clusters discovered in this project, a complete optical follow-up has been carried out.

It is thus not unreasonable to think that such a variety of redshift sources might introduce some undesirable effect particularly on the  $\sigma_v$  estimate and therefore in the final  $L_x - \sigma_v$  relation. To check whether this is the case, we have restricted ourselves to a sample of 38 clusters for which more than seven redshifts per cluster were available, all of them being redshifts measured by us from our own data. This is then to be considered a completely homogeneous sample in terms of both luminosity and redshift, as both quantities have been measured in the same way for all 38 clusters. The result of the ODR fitting is  $\log(L_{45}) = (-0.63 \pm 0.10) + (2.2 \pm 0.4) \log(\sigma_{500})$ . In this case the fit is quite poor, probably because this sample suffers from important selection effects. First, as we have now a small number of data points we should worry about the problems of measuring  $\sigma_v$  with galaxies at small projected distance from the cluster centre, as explained in Section 3.2.

The minimum number of galaxy redshifts set to measure  $\sigma_v$  may have a role too, especially in this case where not too many clusters are available for the fitting. When we consider the whole sample, clusters with a smaller number of individual galaxies are given much less weight into the fit than those with a larger number of observed galaxies. That is not the case here, as all of the clusters show small numbers (only three have more than 15 measured  $z$ ), so the differences in the weights are not so dramatic.

### 5.3 Is this a representative sample from the whole REFLEX catalogue?

Of course, we would like to use all 452 clusters in the REFLEX catalogue to estimate the  $L_x - \sigma_v$  relation. This cannot be done, unfortunately, as the survey was targeted to measure cluster redshifts and not velocity dispersions in these clusters. While multi-object spectroscopy observations were used for a few distant, compact

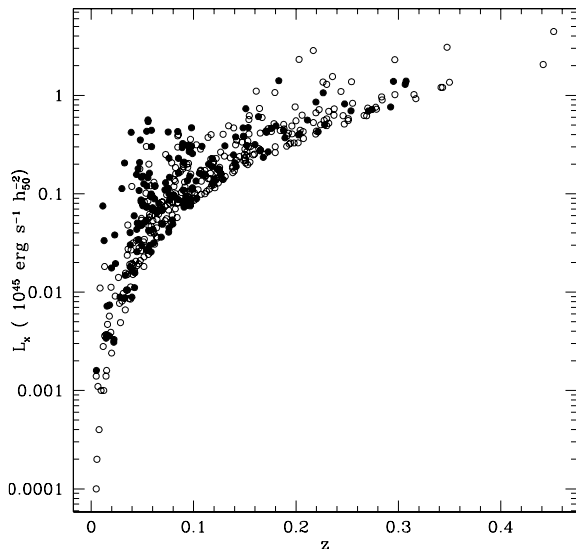


**Figure 7.** The redshift–X-ray luminosity (0.1–2.4 keV) distribution for all clusters in the REFLEX catalogue (open circles) and those from the 81 cluster subsample used in this work (filled circles).

clusters [due to the small field of view, 5 arcmin, of the ESO Faint Object Spectrograph and Camera (EFOSC) on the ESO 3.6-m telescope; see, for example, Guzzo et al. (1999)], providing around 15 redshifts per cluster, most of the new REFLEX cluster redshifts come from (multiple) single slit observations which do not deliver enough galaxy redshifts to compute a velocity dispersion, although the main goal was always to have at least five spectra per target.

We have compared the  $L_x$ – $z$  distribution for the whole catalogue with that corresponding to the 171 cluster subsample used in this work. Fig. 7 shows as filled circles the clusters from the subsample, and as open circles those from the whole REFLEX catalogue. We can see that both samples are approximately equally distributed. The results from a Kolmogorov–Smirnov test are compatible with this conclusion. We find a maximum distance value between the two samples (the entire catalogue and the 171 cluster sample) of 0.11, the probability of this value being larger if coming from a random sample being 0.22.

#### 5.4 Bias from a flux-limited sample: a volume-limited subsample

A bias is expected when measuring the  $L_x$ – $\sigma_v$  relation from a flux-limited sample. Specifically, at the flux cut-off level only the brightest clusters will be considered, for a given velocity dispersion. As our sample has actually been drawn from a flux-limited sample, we may worry about whether we are introducing such a bias towards larger luminosities.

This bias can be avoided by considering a volume-limited subsample. Therefore, we have repeated the analysis for the largest volume-limited sample that we could construct from the 171 cluster sample. It was built by taking all clusters with luminosity  $L_x \geq 0.5 \times 10^{44} h_{50}^{-2} \text{ erg s}^{-1}$ , which corresponds to a redshift limit of  $z_{\text{max}} = 0.08$ . To this redshift the comoving volume surveyed by REFLEX is  $147.4 \times 10^6 h_{50}^{-3} \text{ Mpc}^3$ .

We have a total of 51 ‘useful’ clusters (according to the selection criteria outlined in Section 2) out of the 88 REFLEX clusters in this volume. The ODR fitting gives  $\log(L_{45}) = (-1.20 \pm 0.09) + (3.2 \pm 0.3) \log(\sigma_{500})$ , only compatible at the three-sigma error level with

that obtained from the whole sample, which is an indication of some bias present in the total sample.

## 6 $L_x$ – $T$ AND $\sigma_v$ – $T$ RELATIONS

Another important scaling relation in galaxy clusters is the X-ray luminosity–temperature ( $L_x$ – $T$ ) relation. Again, measurements show that it does not follow the scaling relations predicted by pure gravitational collapse models ( $L_x \propto T^2$ ). The observed  $L_x$ – $T$  relation is closer to  $L_x \propto T^3$  (e.g. Arnaud & Evrard 1999; Reichart, Castander & Nichol 1999; Fairley et al. 2000; Xue & Wu 2000; Novicki, Soring & Henry 2002), which seems to indicate the presence of additional non-gravitational heating sources in the ICM.

$\sigma_v$ – $T$  has also been studied in the literature. There seems to be a consensus in that  $\sigma_v \propto T^{\approx 0.6}$  (see, for example, Lubin & Bahcall 1993; Bird, Mushotzky & Metzler 1995; Girardi et al. 1996; Xue & Wu 2000), again not in agreement with what would be expected in a pure gravitational collapse scenario,  $\sigma_v \propto T^{0.5}$ .

### 6.1 $L_x$ – $T$ and $\sigma_v$ – $T$ in the entire sample

We have studied these relations within our cluster sample to see to which degree our data confirm or otherwise those results. *ASCA* temperatures from two different catalogues (Horner 2001; Ikebe et al. 2002) were used for 54 clusters included in our 171 cluster sample. The measurements of Ikebe et al. were preferred whenever both works had data for the same cluster, as they used a two-temperature model (instead of Horner’s one-component model) for the isothermal plasma, allowing a multiphase ICM, thus obtaining more accurate  $T$  estimates.

Again, we performed the ODR fitting in the log–log space, obtaining the following best-fitting relations (see also Figs 8 and 9):

$$\log(L_{45}) = (-2.53 \pm 0.16) + (3.1 \pm 0.2) \log(T) \quad (7)$$

$$\log(\sigma_{500}) = (-0.45 \pm 0.11) + (1.00 \pm 0.16) \log(T). \quad (8)$$

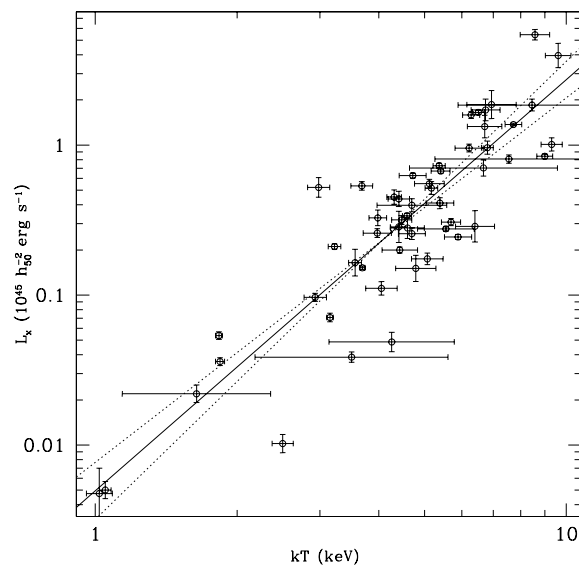


**Figure 8.**  $L_x$ – $T$  for a subsample of 54 clusters drawn from the total sample, for which *ASCA* temperatures were available. The solid line is the ODR best-fitting model, with one-sigma errors marked as dashed lines.

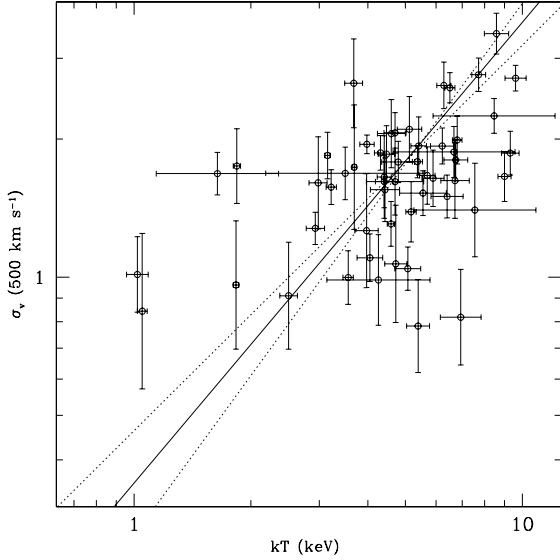


**Figure 9.**  $\sigma_v-T$  for a subsample of 54 clusters drawn from the total sample, for which ASCA temperatures were available. The solid line is the ODR best-fitting model, with one-sigma errors marked as dashed lines.

The  $L_x-T$  estimate that we find is in good agreement (at one-sigma confidence level) with the slope and intercepts previously measured by Fairley et al. (2000) and Arnaud & Evrard (1999).

For the  $\sigma_v-T$  relation, we find here a larger slope than found by other authors (which is  $\approx 0.6$ ). To check that we are not biased for including clusters with substructure in the sample, we select a new set of clusters from the sample in Section 5.1 for which temperature data are available. We have 33 systems, for which we find

$$\log(\sigma_{500}) = (-0.38 \pm 0.13) + (0.92 \pm 0.18) \log(T) \quad (9)$$

in agreement with the previous result. Furthermore, we can select only clusters with the most reliable  $\sigma_v$  determination, that is, those with  $\sigma_v$  measured from more than 30 galaxy redshifts. In doing so, we end up with a sample of 16 clusters, giving

$$\log(\sigma_{500}) = (-0.37 \pm 0.15) + (0.9 \pm 0.2) \log(T). \quad (10)$$

### 6.2 $L_x-T$ and $\sigma_v-T$ in the volume-limited sample

It is interesting to probe these relations also in a volume-limited sample. From the one we constructed in Section 5.4, we select those clusters for which temperature data are available, ending up with a 28 cluster sample. On this we find that

$$\log(L_{45}) = (-2.7 \pm 0.3) + (3.2 \pm 0.4) \log(T) \quad (11)$$

$$\log(\sigma_{500}) = (0.49 \pm 0.05) + (0.77 \pm 0.19) \log(T). \quad (12)$$

$L_x-T$  is still the same, but  $\sigma_v-T$  is flatter than what is found in the 54 cluster sample, steeper than what is expected from self-similar models (at one-sigma confidence level), and in good agreement with what is found by other authors (e.g. Lubin & Bahcall 1993; Girardi et al. 1996; Xue & Wu 2000).

In conclusion, we have derived  $L_x-T$  similar to what is found by previous studies, and which is in contradiction with self-similarity. However, the  $\sigma_v-T$  we are measuring is not reliable, as it has been shown to vary depending on the sample's selection criteria. The scatter and the large error bars in the velocity dispersions make it

impossible to obtain a consistent relation. Still, we can draw a useful conclusion, which is that self-similarity is ruled out in any case.

## 7 SUMMARY AND CONCLUSIONS

We present an estimate of the  $L_x-\sigma_v$  relation computed with a new large and homogeneous sample of clusters from the REFLEX survey. All studies on the  $L_x-\sigma_v$  relation in large samples (with more than  $\approx 100$  clusters) have been performed so far on compilations from the literature requiring the use of models to combine different data from different authors and/or instruments (e.g. Xue & Wu 2000; Mahdavi & Geller 2001).

From the REFLEX catalogue we construct a sample of 171 clusters for which we can derive reliable estimates of  $\sigma_v$ , and then fit the  $\log(L_x)-\log(\sigma_v)$  relation, finding

$$\log(L_{45}) = (-1.34 \pm 0.08) + (4.1 \pm 0.3) \times \log(\sigma_{500}) \text{ erg s}^{-1} h_{50}^{-2}, \quad (13)$$

in agreement with what is expected from self-similar models of cluster formation.

The large size and homogeneity of the sample allows us to make an estimate of the intrinsic dispersion of the  $L_x-\sigma_v$  relation. We find that  $\Sigma_{\text{int}} = 195 \text{ km s}^{-1}$ .

Measurements of  $L_x$  and  $\sigma_v$  in clusters with multiple components may not be reliable. The identification in the literature of those clusters allows us to build a new sample where we remove those with significant substructure in their X-ray emission in Schuecker et al. (2001b). This procedure leaves us with a sample of 123 clusters, on which we fit again the  $\log(L_x)-\log(\sigma_v)$  relation, finding

$$\log(L_{45}) = (-1.28 \pm 0.10) + (4.2 \pm 0.4) \times \log(\sigma_{500}) \text{ erg s}^{-1} h_{50}^{-2}. \quad (14)$$

This is compatible at one-sigma confidence level with the slope and intercept that we find when using the 171 cluster sample, suggesting that the sample is not noticeably affected by clusters with multiple components. The fact that we are considering only galaxies close to the cluster centre may be a reason for that.

We have also investigated the  $L_x-\sigma_v$  relation in a volume-limited sample, finding  $\log(L_{45}) = (-1.20 \pm 0.09) + (3.2 \pm 0.3) \log(\sigma_{500})$ . This significantly flatter slope is an indication that some bias may be present on the whole sample due to the flux limit imposed on the data.

The  $L_x-T$  and  $\sigma_v-T$  scaling relations have also been explored, finding that  $L_x \propto T^{3.1 \pm 0.2}$  and  $\sigma_v \propto T^{1.00 \pm 0.16}$ , in a subsample of 54 clusters for which  $T$  was available from the literature. These results are consistent (within the error bars) with that obtained for  $L_x-\sigma_v$ , as we find  $L_x \propto \sigma_v^{3.1 \pm 0.7}$  when using these  $L_x-T$  and  $\sigma_v-T$  to derive  $L_x-\sigma_v$ .

The slope found in the  $L_x-T$  relationship is steeper than the value predicted by a purely gravitational collapse model of cluster formation, and is in good agreement with previous measurements performed on other cluster samples. As for  $\sigma_v-T$ , the slope we find is only compatible with the self-similar value at the three-sigma confidence level, and slightly larger than the value found by other authors. Also, if we consider a volume-limited sample, the slope found is then in good agreement with previous studies, yet incompatible with self-similarity.

The fact that this model fails to reproduce the measured slope is attributed to the contribution to the ICM energy budget from other non-gravitational heating sources (see, for example, Bialek et al. 2001), such as active galactic nuclei, supernovae, gas cooling (Pearce et al. 2000), the presence of cool cores (Allen & Fabian

1998), or the effect of shocks in cluster formation (Cavaliere, Menci & Tozzi 1997).

Here we are faced with a paradoxical result. The slope of  $L_x-\sigma$  supports the self-similar scenario, whereas  $L_x-T$  and  $\sigma_v-T$  do not, and all three relations are consistent with each other within the one-sigma confidence level. Clearly, more data are required to clarify the situation and reduce the error bars. This is a reflection of the general situation in this topic in the literature. So far, there is a general agreement on  $L_x-T$  and  $\sigma_v-T$ , but there is not such an agreement on  $L_x-\sigma_v$ .

## ACKNOWLEDGMENTS

This work is partially based on observations at the ESO, La Silla, Chile. We thank C. Altucci as her laurea thesis served as a starting point and guideline for this work. We are grateful to the whole REFLEX team which helped in the compilation of this catalogue. We are also indebted to Mrs Yu Xing, who provided us with the data needed to compute the bolometric luminosity out of the luminosity in the *ROSAT* band. We also thank M. Girardi and S. Borgani for stimulating discussions and suggestions. We are indebted to T. Beers who gently provided us with the ROSTAT routines, as well as to the authors of the ODR package, P. Boggs and J. Rogers. PS acknowledges support by the German Aerospace Center (DLR) under the grant No. 50 OR 9708 35. This research has made use of the NED which is operated by the Jet Propulsion Laboratory, California Institute of Technology, under contract with the National Aeronautics and Space Administration (NASA). This research has made use of NASA's Astrophysics Data System.

## REFERENCES

- Allen S. W., Fabian A., 1998, *MNRAS*, 297, L57  
 Anders E., Grevesse N., 1989, *Geochim. Cosmochim. Acta*, 53, 197  
 Andrews D. F., Bickel P. J., Hampel F. R., Rogers W. H., Tuckey J. W., 1972, in *Robust Estimates of Location: Survey and Advances*. Princeton Univ., Princeton, NJ  
 Arnaud K. A., 1996, in Jacoby G., Barnes J., eds, *ASP Conf. Ser. Vol. 101, Astronomical Data Analysis Software and Systems V*. Astron. Soc. Pac., San Francisco, p. 17  
 Arnaud M., Evrard G. E., 1999, *MNRAS*, 305, 631  
 Beers T. C., Flynn K., Gebhardt K., 1990, *AJ*, 100, 32  
 Bialek J. J., Evrard A. E., Mohr J. J., 2001, *ApJ*, 555, 597  
 Bird C., Mushotzky R. F., Metzler C. A., 1995, *ApJ*, 453, 40  
 Böhringer H. et al., 2001, *A&A*, 369, 826  
 Böhringer H. et al., 2002, *ApJ*, 566, 93  
 Boggs P. T., Byrd R. H., Rogers J. E., Schnabel R. B., 1992, NIST IR 4834, US Government Printing Office, Washington DC  
 Borgani S., Rosati P., Tozzi P., Norman C., 1999, *ApJ*, 517, 40  
 Cavaliere A., Menci N., Tozzi P., 1997, *ApJ*, 484, L21  
 Collins C. A. et al., 2000, *MNRAS*, 319, 939  
 Danese L., de Zotti G., di Tullio G., 1980, *A&A*, 82, 322  
 Dell'Antonio I. P., Geller M. J., Fabricant D. G., 1994, *AJ*, 107, 427  
 Edge A. C., Stewart G. C., 1991, *MNRAS*, 252, 428  
 Fairley B. W., Jones L. R., Scharf C., Ebeling H., Perlman E., Horner D., Wegner, G., Malkan M., 2000, *MNRAS*, 315, 669  
 Girardi M., Mezzetti M., 2001, *ApJ*, 548, 79  
 Girardi M., Fadda D., Giuricin G., Mardirossian F., Mezzetti M., Biviano A., 1996, *ApJ*, 457, 61  
 Guzzo L. et al., 1999, *The Messenger*, 95, 27  
 Helsdon S. F., Ponman T. J., 2000, *MNRAS*, 319, 933  
 Horner D., 2001, PhD thesis  
 Ikebe Y., Reiprich T. H., Böhringer H., Tanaka Y., Kitayama T., 2002, *A&A*, 383, 773  
 Kaiser N., 1991, *ApJ*, 383, 104  
 Lubin L., Bahcall N., 1993, *ApJ*, 415, L17  
 Mahdavi A., Böhringer H., Geller M. J., Ramella M., 2000, *ApJ*, 534, 114  
 Mahdavi A., Geller M. J., 2001, *ApJ*, 554, L129  
 Mulchaey J. S., Zabludoff A. I., 1998, *ApJ*, 496, 73  
 Novicki M. C., Sornig M., Henry J. P., 2002, *AJ*, 124, 2413  
 Pearce F. R., Thomas P. A., Couchman H. M. P., Edge A. C., 2000, *MNRAS*, 317, 1029  
 Quintana H., Melnick J., 1982, *AJ*, 87, 972  
 Reichart D. E., Castander F. J., Nichol R. C., 1999, *ApJ*, 516, 1  
 Schuecker P. et al., 2001a, *A&A*, 368, 86  
 Schuecker P., Böhringer H., Reiprich T. H., Feretti L., 2001b, *A&A*, 378, 408  
 Schuecker P., Böhringer H., Collins C. A., Guzzo L., 2003a, *A&A*, 398, 867  
 Schuecker P., Caldwell R. R., Böhringer H., Collins C. A., Guzzo L., Weinberg N. N., 2003b, *A&A*, 402, 53  
 Solinger A. B., Tucker W. H., 1972, *ApJ*, 175, L107  
 Wainer H., Thissen D., 1976, *Psychometrika*, 41, 9  
 White D. A., Jones C., Forman W., 1997, *MNRAS*, 292, 419  
 Xue Y.-J., Wu X.-P., 2000, *ApJ*, 538, 65

This paper has been typeset from a  $\text{\TeX}/\text{\LaTeX}$  file prepared by the author.